

## Top-quark properties at Tevatron with the CDF detector

M. DATTA

*Fermi National Accelerator Laboratory - Batavia (IL), USA*

(ricevuto l'1 Ottobre 2010; approvato l'1 Ottobre 2010; pubblicato online il 15 Novembre 2010)

**Summary.** — In this paper we present the latest results on the measurements of top-quark properties from the CDF Collaboration. Studies of top-quark properties provide a test of the Standard Model (SM) and work as a probe for possible physics beyond the SM. Results presented here use up to  $4.3 \text{ fb}^{-1}$  Tevatron Run II data and are some of the most precise measurements of the top-quark properties to date.

PACS 14.65.Ha – Top quarks.

### 1. – Introduction

The top quark is the most massive fundamental particle observed by experiment. The existence of the top quark is predicted by the SM. The top quark ( $T_3 = +1/2$  and  $Q = 2/3$ ) is the weak iso-spin partner of the bottom quark. The mass of the top quark  $m_t$  is about  $173 \text{ GeV}/c^2$  [1], which is much larger than the masses of all the other quarks and is in the same order of magnitude as the masses of  $W$  and  $Z$  bosons. The large mass makes top-quark properties unique and interesting both from the viewpoint of the SM and beyond. Due to the large mass the top quark lifetime in the SM is expected to be about  $0.5 \times 10^{-24} \text{ s}$ . As a result unlike any other quark the top quark in the SM decays before hadronization [2], providing us with the unique opportunity to study the properties of a “bare” quark. Furthermore, the top quark might provide insight to electroweak (EW) symmetry-breaking mechanism and could be a probe to beyond the SM (BSM) physics.

Top quark was discovered in 1995 by the CDF and D0 experiments at the Fermilab Tevatron during the Run I operation [3]. Since the start of the Tevatron Run II in 2001, both the CDF and D0 experiments have collected  $\sim 7 \text{ fb}^{-1}$  data samples, which are over seventy times larger than that used in the Run I discovery. This larger data sample allows more precise measurement of the top-quark properties.

## 2. – Top quark production and decay

In the hadron collisions top quarks are predominantly produced in pairs through the QCD processes  $q\bar{q} \rightarrow t\bar{t}$  and  $gg \rightarrow t\bar{t}$ . For Tevatron Run II at  $\sqrt{s} = 1.96$  TeV the expected  $t\bar{t}$  production cross section is  $\sigma_{t\bar{t}} = 7.45^{+0.72}_{-0.63}$  pb [4] for  $m_t = 172.5$  GeV/ $c^2$ . Top quark can also be produced in hadron collisions singly through EW processes. The cross sections for single top production in  $s$ -channel and  $t$ -channel at  $\sqrt{s} = 1.96$  TeV are  $0.88 \pm 0.11$  pb and  $1.98 \pm 0.25$  pb, respectively [5] for  $m_t = 175$  GeV/ $c^2$ .

In the SM top quark decays to a  $W$  boson and a  $b$  quark most of the time. The  $t\bar{t}$  final states are divided into three channels based on the decay mode of the two  $W$  bosons: i) dilepton:  $t\bar{t} \rightarrow W^+bW^-\bar{b} \rightarrow \bar{\ell}\nu_\ell b\ell'\bar{\nu}_{\ell'}\bar{b}$ , branching ratio  $\sim 10\%$ , relatively low background; ii) lepton+jets:  $t\bar{t} \rightarrow W^+bW^-\bar{b} \rightarrow q\bar{q}'b\ell\bar{\nu}_{\ell'}\bar{b} + \bar{\ell}\nu_\ell b q\bar{q}'\bar{b}$ , branching ratio  $\sim 43\%$ , medium background level; and iii) all hadronic:  $t\bar{t} \rightarrow W^+bW^-\bar{b} \rightarrow q\bar{q}'bq''\bar{q}'''\bar{b}$ , branching ratio  $\sim 46\%$ , suffers from large QCD background. Here  $\ell = e, \mu, \text{ or } \tau$ , though most of the lepton+jets and dilepton analyses rely only on the  $e$  and  $\mu$  decay modes.

## 3. – The CDF detector

The measurements are based on a data set with an integrated luminosity of up to  $4.3\text{fb}^{-1}$  acquired by the Collider Detector at Fermilab (CDF II) from ppbar collisions at  $\sqrt{s} = 1.96$  TeV. The CDF II detector is a general-purpose particle detector and is described in detail elsewhere [6]. It has a solenoidal charged particle spectrometer, consisting of 7-8 layers of silicon microstrip detectors and a cylindrical drift chamber immersed in a 1.4 T magnetic field, a segmented sampling calorimeter, and a set of scintillators and drift tubes outside the calorimeter used to identify muon candidates. We use a right-handed cylindrical coordinate system with the origin in the center of the detector, where  $\theta$  and  $\phi$  are the polar and azimuthal angles, respectively, and pseudorapidity is defined as  $\eta \equiv -\ln \tan(\theta/2)$ . Transverse energy and momentum are  $E_T = E \sin \theta$  and  $p_T = p \sin \theta$ , respectively, where  $E$  and  $p$  are energy and momentum.

## 4. – Recent results

This section discusses some of the recent results on top-quark physics from the CDF experiment [7]:

- Forward-backward asymmetry ( $A_{fb}$ ) in top pair production [8],
- $A_{fb}$  dependence on the invariant mass of  $t\bar{t}$  [9],
- Measurement of the  $t\bar{t}$  differential cross section  $d\sigma/dM_{t\bar{t}}$  [10],
- Measurement of  $W$ -boson polarization from top-pair decay [11],
- Measurement of top-quark width [12],
- Measurement of top-quark charge [13],
- Measurement of EW single-top polarization [14].

Besides single-top polarization measurement, all the analyses are done using lepton+jets final state. The lepton+jets event selection and expected sample compositions are based on  $t\bar{t}$  cross section measurement in that channel [15]. The basic lepton+jets

selection for top-quark properties measurement requires a single high- $p_T$  electron or muon in the central portion of the detector ( $|p_T| > 20 \text{ GeV}/c$  and  $|\eta| < 1.1$ ), a large amount of missing transverse energy ( $MET > 20 \text{ GeV}$ ) and four or more high- $E_T$  jets ( $|E_T| > 20 \text{ GeV}/c$  and  $|\eta| < 2.0$ ). To improve the relative signal-to-background ratio we require at least one of the jets to have originated from a  $b$  quark by using an algorithm that identifies a long-lived  $b$  hadron through the presence of a displaced vertex (SecVtx  $b$  tag). The techniques for the reconstruction of the kinematics of  $t\bar{t}$  events are described in details in [16]. The two techniques that are commonly used are i)  $\chi^2$  based kinematic fitter and ii) a likelihood technique based on the theoretical matrix elements for the  $t\bar{t}$  production and decay.

Brief descriptions of the analyses are as follows.

**4.1. Forward-backward asymmetry  $A_{fb}$  in top quark production.** – An integral charge asymmetry, which is equivalent to a forward-backward asymmetry  $A_{fb}$  in the  $CP$  invariant Tevatron system, compares the number of top and anti-top quarks produced with momentum in a given direction. The measurement described in this proceeding is based on  $3.2 \text{ fb}^{-1}$  of CDF data. In the SM a small charge asymmetry,  $A_{fb} = 0.050 \pm 0.015$  in  $p\bar{p}$  frame, arises due to interference of initial-state radiation diagrams with final-state diagrams. However, BSM physics such as  $Z'$ -like states with parity violating coupling or theories with chiral color can significantly enhance the asymmetry.

We measure  $A_{fb}$  in  $p\bar{p}$  frame and use the laboratory direction of the hadronically decaying top (or anti-top) system from the lepton+jets channel. To obtain  $A_{fb}$  we assume  $CP$  invariance and measure the asymmetry in  $-Q_\ell \cdot Y_{\text{had}}$ ,

$$(1) \quad A_{fb} = \frac{N(Q_\ell \cdot Y_{\text{had}} > 0) - N(Q_\ell \cdot Y_{\text{had}} < 0)}{N(Q_\ell \cdot Y_{\text{had}} > 0) + N(Q_\ell \cdot Y_{\text{had}} < 0)},$$

where  $Y_{\text{had}}$  is the rapidity of the hadronically decaying system and  $Q_\ell$  is the charge of the lepton of the leptonically decaying system.

To obtain the production angle of the top quark, we reconstruct the complete kinematics of the  $t\bar{t}$  final state using a  $\chi^2$ -based kinematic fitter. The jet-parton assignment that gives the lowest  $\chi^2$  value is used for reconstructing the  $Q_\ell \cdot Y_{\text{had}}$ . We subtract expected backgrounds from the  $Q_\ell \cdot Y_{\text{had}}$  distribution in data, and perform a model-independent correction for acceptance and reconstruction dilutions in order to find the asymmetry which can be compared with theoretical predictions. Using  $3.2 \text{ fb}^{-1}$  the measured forward-backward asymmetry in the  $p\bar{p}$  frame is

$$A_{fb} = 0.193 \pm 0.065(\text{stat}) \pm 0.024(\text{sys}).$$

The reconstructed  $-Q_\ell \cdot Y_{\text{had}}$  distribution is shown in fig. 1, using signal template corresponding to the measured  $A_{fb}$  value in data. The measured central value deviates from the theory prediction at about two standard deviation levels. Measurements with larger data sample are required to revolve this potentially interesting deviation.

**4.2.  $A_{fb}$  dependence on the invariant mass of  $t\bar{t}$ .** – In addition to measuring the integral  $A_{fb}$  CDF has also performed a measurement of the  $A_{fb}$  dependence on invariant mass  $M_{t\bar{t}}$  of the top pair system, which is another natural way to look for a new top pair production channel. The result is presented as a scan of the  $A_{fb}$  in the  $p\bar{p}$  frame below and above eight different  $M_{t\bar{t}}$  thresholds values ranging from 400 to 800  $\text{GeV}/c^2$ . Using an unfolding technique, we unsmear the effects of the reconstruction back to parton

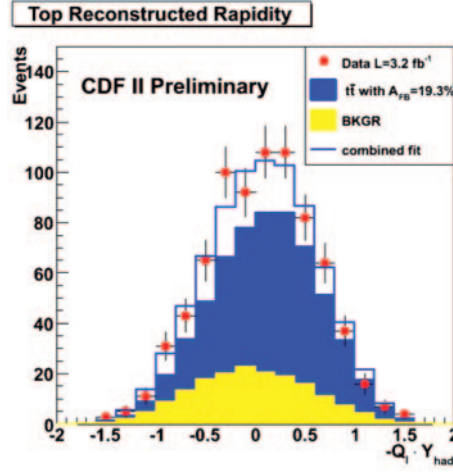


Fig. 1. – The  $-Q_\ell \cdot Y_{\text{had}}$  distribution from data compared with backgrounds, and signal template corresponding to  $A_{fb} = 19.3\%$ .

level simultaneously in the  $Q_\ell \cdot Y_{\text{had}}$  and  $M_{t\bar{t}}$  variables. Figure 2 shows the distributions for reconstructed  $M_{t\bar{t}}$  (left plot) for events with positive and negative values of  $Q_\ell \cdot Y_{\text{had}}$ :  $Q_\ell \cdot Y_{\text{had}} > 0$  (FW) and  $Q_\ell \cdot Y_{\text{had}} < 0$  (BW), and  $A_{fb}$  versus  $M_{t\bar{t}}$  for events above the invariant mass edges shown by the  $x$ -axis (right plot). The results are consistent with a recent Next-to-Leading-Order (NLO) calculation.

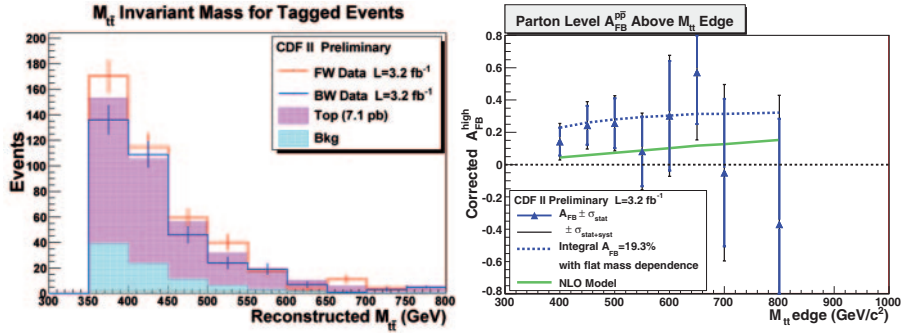


Fig. 2. – (Colour on-line) Shown are the distributions for reconstructed  $M_{t\bar{t}}$  (left plot) for FW and BW events, and  $A_{fb}$  vs.  $M_{t\bar{t}}$  for events above the invariant mass edges shown by the  $x$ -axis (right plot). In the left plot data (points) are superimposed to the sum of  $t\bar{t}$  MC generated using PYTHIA (pink histogram) and background (light blue histogram). The PYTHIA  $t\bar{t}$  sample contains null  $A_{fb}$ . For simplicity, the MC predictions are normalized to half of the predicted value for a sample of  $3.2\text{fb}^{-1}$  integrated luminosity. For the right plot, the data point with error bars are the central value returned by the two-variable unfold; the inner error bars are the statistical uncertainties as returned by the unfold; the outer bars are the sum of the statistical and systematic uncertainties. The dashed line corresponds to a template of null  $dA_{fb}/dM_{t\bar{t}}$  and an integral  $A_{fb} = 19.3\%$ . The green solid line shows the results for a model with  $dA_{fb}/dM_{t\bar{t}} = 2.5\%$  and  $A_{fb} = 3\%$  as derived from the fit to the NLO calculation.

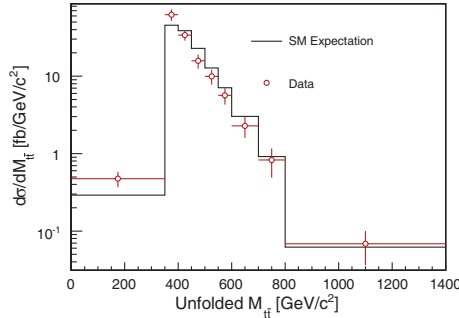


Fig. 3. –  $d\sigma/dM_{t\bar{t}}$  distribution in data compared with the SM prediction.

**4.3. Measurement of the  $t\bar{t}$  differential cross section  $d\sigma/dM_{t\bar{t}}$ .** – Various BSM models predict additional heavy gauge bosons that couple strongly to top quark, which can distort the  $t\bar{t}$  invariant mass  $M_{t\bar{t}}$  spectrum relative to the SM expectation. CDF has performed the first measurement of the  $t\bar{t}$  differential cross section with respect to the  $t\bar{t}$  invariant mass,  $d\sigma/dM_{t\bar{t}}$ . This measurement is potentially sensitive to broad enhancements of the spectrum and interference effects, as well as to narrow  $t\bar{t}$  resonances.

The analysis uses  $2.7\text{ fb}^{-1}$  CDF data and selects events in lepton+jets channel. The precision of the measurement of  $M_{t\bar{t}}$  depends on the uncertainties from jet energy scale (JES) determination, which is reduced by using the measured invariant mass of the hadronically decaying  $W$  boson to constrain the JES. We reconstruct  $M_{t\bar{t}}$  for the event using the four-vectors of the  $b$ -tagged jet, the three remaining leading jets, the lepton and the MET. The  $M_{t\bar{t}}$  distribution is divided into nine bins between 0 and  $1400\text{ GeV}/c^2$  with bin widths chosen based on expected number of events. After subtracting the expected backgrounds contribution from the reconstructed  $M_{t\bar{t}}$  we extract the true underlying  $M_{t\bar{t}}$  distribution through a response matrix  $A$  that maps between the true ( $x$ ) and measured ( $d$ ) binned distributions  $Ax = d$ . A singular-value decomposition unfolding method is used to properly handle the potential issues during matrix inversion due to statistical fluctuations in bins with small numbers of events.

The measured  $d\sigma/dM_{t\bar{t}}$  is shown in fig. 3. The consistency with the SM prediction is checked using the Anderson-Darling statistics and no evidence of non-SM physics was found. Further by looking for graviton resonances in the  $t\bar{t}$  invariant mass spectrum predicted by the Randall-Sundrum model, where the mass of the first graviton mode is fixed at  $600\text{ GeV}/c^2$ , we set limits on  $\kappa/M_{\text{Pl}} > 0.16$  at the 95% confidence level (CL).

**4.4. Measurement of  $W$ -boson polarization from top-pair decay.** – The top quark in the SM decays via the charged current weak interaction predominantly to a  $W$  boson and a  $b$  quark, with the  $W$  decaying into quarks (an up-type quark and a down-type quark) or leptons (a charged lepton and a neutrino). The coupling at the  $Wtb$  vertex is purely left-handed and can be used to test the  $V - A$  structure of the weak interaction. In the SM the fractions for longitudinally  $f_0$ , left-handed  $f_-$  and right-handed  $f_+$   $W$  bosons from top decays are predicted to be 0.7, 0.3 and 0.0, respectively. The SM expectation might be modified due to the presence of anomalous couplings.

The measurement described in this proceeding is based on  $2.7\text{ fb}^{-1}$  of CDF data and uses a matrix element method. We express the matrix element in terms of the  $W$ -boson polarization fractions and the cosine of the angle  $\theta^*$  between the momentum of the

charged lepton or down-type quark in the  $W$ -boson rest frame and the momentum of the  $W$  boson in the top-quark rest frame.

We report measurements of the  $W$ -boson polarization for three different hypotheses of top-quark decay:

- i) Model-independent with simultaneous measurement of  $f_0$  and  $f_+$ :

$$\begin{aligned} f_0 &= 0.879 \pm 0.106(\text{stat}) \pm 0.062(\text{syst}), \\ f_+ &= -0.151 \pm 0.067(\text{stat}) \pm 0.057(\text{syst}). \end{aligned}$$

The statistical correlation between  $f_0$  and  $f_+$  is  $\rho = -0.59$ .

- ii) Anomalous tensor couplings with measurement of  $f_0$  for fixed  $f_+ = 0$ :  $f_0 = 0.701 \pm 0.069(\text{stat}) \pm 0.041(\text{syst})$ ; and
- iii) Anomalous right-handed couplings with measurement of  $f_+$  for fixed  $f_0 = 0.70$ :  $f_+ = -0.010 \pm 0.019(\text{stat}) \pm 0.049(\text{syst})$  and find  $f_+ < 0.12$  at 95% CL.

All the measurement are in consistent with the SM expectation.

**4.5. The measurement of EW single top polarization.** – The Tevatron experiments have recently observed the single top quark production [17]. In the SM this process proceeds via EW interaction and the single-top quarks expected to be approximately 100% polarized. However the polarization fraction can be modified due to the presence of BSM production mechanisms or anomalous  $tWb$  couplings.

The analysis tests an alternative model in which the top quarks are produced with opposite polarization compared to the SM, however they decay according the SM (RLL). The measurement is performed based on  $3.2 \text{ fb}^{-1}$  data using top decay channels with leptonically ( $e$  or  $\mu$ ) decaying  $W$ . We look at the distributions of the cosine of the angle between the lepton and the down-type quark,  $\cos\theta_{\ell j}$ , in the top quark reference frame. In order to measure separately the RLL and SM signals, the sample is divided into two subsets:  $\cos\theta_{\ell j} > 0$  and  $\cos\theta_{\ell j} < 0$ . Event selection and sample composition is described in details in [17]. A likelihood discriminant is used to separate the signals from the backgrounds, which is trained separately on the two subsets to measure the cross section as independently as possible.

A two-dimensional fit is performed to simultaneously obtain the SM and RLL cross sections, using the same technique used for the single top  $s$ - and  $t$ -channel production cross section measurements. The results for the two-dimensional fit is shown in fig. 4. The best-fit values for SM cross section  $\sigma_L = 1.72 \text{ pb}$  and for RLL cross section  $\sigma_R = 0.0 \text{ pb}$ . The measured polarization  $P = \frac{\sigma_R - \sigma_L}{\sigma_R + \sigma_L} = -1_0^{+1.5}$ . The result is consistent with the SM prediction.

**4.6. A measurement of top quark width in lepton+jets channel.** – In the SM the total width of the top quark is calculated to a precision of about 1%; it is approximately 1.5 GeV. Measurement of top width provides a general way to rule out the presence of a large top quark decay rate to non-SM channels, including those with non-detectable final states. The measurement is based on  $4.3 \text{ fb}^{-1}$  of CDF data and a template method used for top-quark mass measurement [18]. The two-dimensional distributions of reconstructed top mass  $m_t^{\text{reco}}$  and the invariant mass of the jets coming from the hadronically decaying  $W$  boson  $m_{jj}$  from data are compared to Monte Carlo (MC) to extract the top

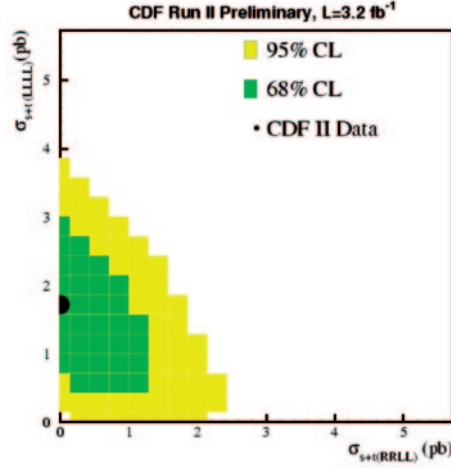


Fig. 4. – Two-dimensional fit for obtaining SM and RRLC cross sections.

quark width using maximum likelihood fit. The  $t\bar{t}$  MC samples with different input top widths ranging from 0.1 GeV to 30 GeV are generated using the same input top quark mass of  $172.5 \text{ GeV}/c^2$ . Using pseudo experiments for different top width Feldman-Cousins bands for top quark width are constructed which is used to set limit on top-quark width.

From the data fit result we set an upper limit on the top quark width of  $\Gamma_{\text{top}} < 7.6 \text{ GeV}$  at 95% CL, which corresponds to a lower limit on the top quark lifetime of  $\tau_{\text{top}} > 8.7 \times 10^{-26} \text{ s}$  at 95% CL. We also set central limits of top width at 68% CL  $0.3 \text{ GeV} < \Gamma_{\text{top}} < 4.4 \text{ GeV}$ .

**4.7. Exclusion of exotic top-like quark with  $-4/3$  electric charge using soft lepton tags (SLT).** – The SM predicts the charge of the top quark to be  $+2/3$ . Most of the measurements using  $t\bar{t}$  events pair a  $W$  with a  $b$ -quark. For  $W \rightarrow \ell\nu$ , the charge of the  $W$  is known from the charge of the lepton. However, we do not distinguish between a  $b$ -quark and  $\bar{b}$ -quark. Therefore, the charge of the  $Wb$  pair can be  $+2/3$  or  $-4/3$ . It has been postulated that the observed quark with mass  $\sim 173 \text{ GeV}/c^2$  has a charge of  $-4/3$  and is a different particle, called “XM top”, and the true “SM top” is massive enough to escape detection.

The analysis described in this document is based in  $2.7 \text{ fb}^{-1}$  of CDF data. Events are selected in the lepton+jets channel. In order to increase acceptance for  $t\bar{t}$  events the fourth jet is allowed to pass a looser selection ( $E_T > 12 \text{ GeV}$  and  $|\eta| < 2.4$ ). Further we require one of the tight jets must be tagged as a b-jet by either  $SLT_{e/\mu}$  or SecVtx algorithms.

The two main components to top charge measurement are as follows:

- Identifying the b-quark associated with either the leptonically decaying  $W$  (leptonic  $b$ ) or hadronically decaying  $W$  (hadronic  $b$ ): A kinematic fitter is used to determine which b-jet is leptonic and which is hadronic. The kinematic reconstruction can correctly assign the b-jets for approximately 76% of the events.
- Determining its flavor, either  $b$  or  $\bar{b}$ : The SLT taggers are used to determine the b-jet flavors, which is preserved through the semileptonic decay  $b \rightarrow \ell^- \bar{\nu} X$ . The SLT

method is much less efficient since the semileptonic branching fraction for b-jets is only approximately 10%; however, the purity  $P$  of the SLT taggers at flavor reconstruction is approximately 71%. Therefore we can still achieve a reasonable sensitivity  $\varepsilon D^2$ , where  $\varepsilon$  is the efficiency for SLT tag,  $D = 2P - 1$  is the dilution and  $P$  is the purity.

Each event is considered SM if the charge of lepton from  $W$  and the charge of the leptonic (hadronic) b-jet are the opposite (same); otherwise the event is considered to contain XM top (XM). This binary event reconstruction implies that if both the kinematic fitter and the SLT tagger are incorrect, then the correct top charge is still reconstructed. The method correctly reconstructs the top charge in  $\sim 61\%$  of events. The measurement of the purity of the charge reconstruction for both  $t\bar{t}$  and backgrounds is carried out with MC simulation; we calibrated it with a data-driven technique and where we measure a dilution scale factor in a sample of pure  $b\bar{b}$  events.

We construct an asymmetry  $A$  based on numbers SM-like events  $N_{\text{SM}}$  and XM-like events  $N_{\text{XM}}$ :

$$A \equiv \frac{1}{D_s} \frac{N_{\text{SM}} - N_{\text{XM}} - \langle B \rangle D_B}{N_{\text{SM}} - N_{\text{XM}} - \langle B \rangle},$$

where  $D_S$  and  $D_B$  are the signal and background dilutions, respectively, and  $\langle B \rangle$  is the total background expectation. When we reconstruct the top charge in data, we measure 45 total events, of which 29 are reconstructed as SM and 16 are reconstructed as XM. We derive a SM and XM  $p$ -values,  $p_{\text{SM}}$  and  $p_{\text{XM}}$  using pseudo-experiments. The measured  $p$ -values are  $p_{\text{SM}} = 0.69$  and  $p_{\text{XM}} = 0.0094$ , while the median  $p$ -values assuming SM are  $p_{\text{SM}} = 0.50$  and  $p_{\text{XM}} = 0.028$ . The type-I error rate  $\alpha$  is chosen *a priori*, by using the standard threshold for exclusion of SM  $\alpha = 0.05$ . Based on that we exclude the exotic  $-4/3$  charged top quark at 95% confidence level.

## 5. – Conclusion

The recent results from the measurements for top-quark properties from the CDF experiment are presented. All the measurement presented here are limited by statistics. The Tevatron has much larger  $t\bar{t}$  sample compared to that in Run I. However  $\sim 4 \text{ fb}^{-1}$  data sample consists of about few thousand reconstructed signal events. By the end of 2010 CDF is expected to have  $8.5 \text{ fb}^{-1}$  data recorded and the Tevatron will still offer the world's largest  $t\bar{t}$  sample for analyses. Most of the analysis will be updated with the increasing dataset. Further the results from the CDF and D0 experiments will be combined. For some of the top-properties measurements Tevatron combination based on full dataset will become systematically limited. Tevatron's top physics program and understanding of systematic effects will continue to play a significant role for years to come.

## REFERENCES

- [1] TEVATRON ELECTROWEAK WORKING GROUP for the CDF and DØ COLLABORATIONS, FERMILAB-TM-2466-E, TEVEWWG/top 2010/07, CDF Note 10210, D0 Note 6090 (2010).
- [2] BIGI I. *et al.*, *Phys. Lett. B*, **181** (1986) 157.



- [3] ABE F. *et al.* (CDF COLLABORATION), *Phys. Rev. Lett.*, **74** (1995) 2626; ABACHI S. *et al.* (D0 COLLABORATION), *Phys. Rev. Lett.*, **74** (1995) 2632.
- [4] MOCH S. and UWER P., *Nucl. Phys. Proc. Suppl.*, **183** (2008) 75.
- [5] SULLIVAN Z., *Phys. Rev. D*, **70** (2004) 114012.
- [6] ACOSTA D. *et al.* (CDF COLLABORATION), *Phys. Rev. D*, **71** (2005) 031101(R).
- [7] <http://www-cdf.fnal.gov/physics/new/top/top.html>
- [8] AALTONEN T. *et al.* (CDF COLLABORATION), CDF note 9724 (2009).
- [9] AALTONEN T. *et al.* (CDF COLLABORATION), CDF note 9853 (2009).
- [10] AALTONEN T. *et al.* (CDF COLLABORATION), *Phys. Rev. Lett.*, **102** (2009) 222003.
- [11] AALTONEN T. *et al.* (CDF COLLABORATION), *Phys. Rev. Lett.*, **105** (2010) 042002.
- [12] AALTONEN T. *et al.* (CDF COLLABORATION), CDF note 10035 (2010).
- [13] AALTONEN T. *et al.* (CDF COLLABORATION), CDF note 9939 (2010).
- [14] AALTONEN T. *et al.* (CDF COLLABORATION), CDF note 9920 (2009).
- [15] DELIOT F., these proceedings.
- [16] CANELLI F., these proceedings.
- [17] LUECK J., these proceedings.
- [18] BRANDT O., these proceedings.